EUV lithography patterning using Multi-Trigger Resist

C. Popescu[a], G. O'Callaghan[a], A. McClelland[a], C. Storey[a], J. Roth[b], E. Jackson[b], A.P.G. Robinson[a,c]

[a]Irresistible Materials, Birmingham Research Park, Birmingham, UK
[b]Nano-C, 33 Southwest Park, Westwood, MA, USA
[c] School of Chemical Engineering, University of Birmingham, B15 2TT, UK

e-mail: a.p.g.robinson@bham.ac.uk

Keywords: EUV lithography, photoresist, molecular resist, multi-trigger resist, chemical amplification, crosslinking

ABSTRACT

Irresistible Materials is developing a novel photoresist for EUV lithography including high-NA patterning. A major concern for the key research area of high-NA EUV resists is that stochastics in such resist materials can lead both to roughness and defects causing failures, which means high-NA resists remain a priority research area. We are developing a photoresist based on the multi-trigger concept, which seeks to suppress line edge roughness using a new photoresist mechanism, and which is based on molecular rather than polymeric materials to maximize resolution. It also has relatively high EUV absorbance to increase photon capture despite the need for thin films in high-NA due to limited depth-of-focus.

By modifying the MTM molecule, crosslinker and PAG, both individually and in combination, we can optimize the reaction rates in the MTR mechanism. Different combinations have been designated Gen 2.1 to Gen 2.6 and show an LWR improvement in Gen 2.4, 2.5 and 2.6 combinations. Here we present the lithographic performance at pitch 28nm dense line/space where 14.1 wide lines were patterned at 59 mJ/cm^2 with an unbiased LER of 2.09 nm using a Gen 2.4 resist. We show hexagonal pillar results: pitch 32 nm patterned at 42 mJ/cm^2 to obtain a pillar diameter of 16 nm with an unbiased LCDU of 2.8 nm; and additionally p32 pillars of 16 nm diameter were patterned at 74 mJ/cm^2 with an unbiased LCDU of 2.7nm; and of 18.5 nm diameter at 82 mJ/cm^2 with an unbiased LCDU of 2.3nm. We also show data which shows using a Gen 2.6 resist can reduce the LCDU of p32 hex pillars by 0.2 nm and biased LWR of p28 l/s by 0.3 nm compared to a comparable Gen 2.4 resist.

Performance improvements such as reduced roughness and defectivity can also be shown to be affected by choices such as underlayer and developer. Additionally, the modification of the developer can be shown to influence the patterning performance of the resist at high resolution.

1. INTRODUCTION

The search for suitable resist materials to support the next generation EUV lithography, including the implementation of high-NA lithography, continues. It is generally accepted that development of new photoresist mechanisms is required as existing chemically amplified resists (CAR) will be unable to pattern the tightest pitches, and thus non-chemically amplified resists (non-CAR) are drawing more attention than ever before. Specifically, CARs are expected to reach a plateau in performance when it comes to simultaneously achieving the ultimate resolution, low line edge roughness, high sensitivity and low defectivity required in high-NA, and so progress in non-CAR materials is necessary. [1–3] However, there remain many unknowns, which are slowing this development, most important being the mechanism by which the EUV photons interact within the photoresist film.

The prevalence of high energy photons in EUV lithography has shifted the photoresist chemistry towards secondary electron chemistry, with the prospect of a interesting space for novel resist mechanisms to be developed. However, the details of the interactions of low energy electrons with resist molecules are not entirely understood and the chemical events

involved in the resist mechanism are still being researched. [4] Various models of photo-acid generation have been proposed to explain the interactions taking place within photoresists during EUV exposures. Most studies focused on the possibility that multiple ionization events are followed by electron recombination with PAG molecules leading either directly [5] or indirectly [6] to acid generation. More recent work led by Brainard and co-workers, however, suggests an alternative mechanism based on internal excitations contributing to acid generation. [4,7]

Underlayer choice can also play a very important role in the overall performance of resists. The events occurring at the interface between the photoresist and the silicon wafer are modulated by the chemical composition and the physical properties of the underlayer. These events can contribute beneficially or detrimentally towards resolution and roughness in the features patterned, for instance by modulating the resist adhesion. The generation of secondary electrons in the underlayer may also be important. [8,9] Furthermore, the underlayer choice also affects the metrology introducing contrast variations, depending on the underlayer used, in non-intuitive ways. [10] Finally, as industry moves towards the implementation of high-NA EUV to enable further improvements in resolution, it will become increasingly important to consider the overall thickness of the resist/ underlayer stack. It has long been known that the achievable post development film thickness has needed to reduce, as pitch sizes decrease, to avoid pattern collapse, [11] and that this trend is accelerating [12]. However, film thicknesses will be further suppressed in high-NA, as the depth of focus of the tool is known to be severely constrained. [13] The metrology issues will also be exacerbated, and optimisation of the underlayer/ photoresist stack will need to increase, whilst ever thinner photoresists will also introduce pattern transfer challenges. [14]

Irresistible Materials have developed the multi trigger resist (MTR) material to address the on-going requirements of EUV lithography. The MTR material is a molecular resist, which utilises ring-opening polymerisation (ROP) and incorporates a unique self-quenching mechanism, known as the multi-trigger mechanism, directly in the chemical pathways, to improve performance. The intrinsic self-quenching mechanism in the MTR material, which has been described before [15–21] provides an advantage in acid diffusion mitigation and offers a benefit on achieving ultimate resolutions with low edge roughness. After the development of the initial prototype of the resist, MTR Generation 1 (Gen1) was developed, incorporating non-metal organic high-opacity moieties for high photo-absorption. MTR Gen1 is additionally a high-carbon content material with a low Ohnishi number, and shows low post development film thickness loss (~10–20%). Transfer of lines and pillar patterns from MTR films using SiN as a hard mask and standard etch processes, even from thin films (26 nm post-coat; 24 nm post-development) has been demonstrated. [22]

MTR Generation 2 (Gen2) was introduced in 2022, and initial results were presented. [19] In particular, we showed that good lithographic performance for P28 L/S with doses below 20 mJ/cm^2 and p36 and p34 hexagonal pillars with doses below 30 mJ/cm^2. [22, 23] More recently we have explored three separate routes to significantly improve the Z-factor of the MTR system, either by increasing the activation rate of the monomer activation (Gen2.1); adjusting the relative reaction rates of the initiation and propagation rates of the ROP (Gen2.2); and via a more efficient multi-trigger quenching mechanism (Gen2.3). Additionally, the advantages gained by each approach are not correlated, and thus can be combined for further improvements of the MTR Z-factor (Gen2.4 and Gen 2.5) [24, 25]. Here we present new data showing the improvement shown by Gen 2.4, and also Gen 2.6, where all three improvement routes are combined.

2. EXPERIMENTAL

The resist samples were prepared by dissolving the individual components in ethyl lactate. The solutions are combined in various weight ratios and concentrations to give a range of formulations. The solutions undergo metal ion removal using 3M Zeta Plus filtration disks to reduce metals to levels appropriate for fab based processing.

The resist was spun onto a commercial organic underlayer, Brewer Scientific Optistack® AL412, unless stated. After spin-coating of the resist the samples received a post application bake (PAB) of 80°C for 1 minute, using a track for film deposition, and the samples were exposed to EUV using an ASML NXE3400 scanner at imec. After exposure the samples received a post exposure bake of 65°C unless stated and were developed in Fujifilm DP819A developer for 30 seconds using a dynamic system with no subsequent rinse. The patterning was observed using a Hitatchi CD-SEM (model 5000, 6300 or GT2000) and the LWR, LER, and LCDU values are biased values as measured inline unless otherwise stated. For select wafers, MetroLER analysis using an appropriate number of images (25 for pillars, 50–100 for p28 lines) at each dose was carried out to calculate unbiased LWR, LER and LCDU numbers, and also calculate the defectivity (e.g. merged or missing pillars) for the sample.

The baseline for the optimization is the previously introduced xMT resist system [15–21], from which the MTR Gen 1 series resist was developed. The molecular resin has been modified, to increase glass transition temperature (T_g) and to optimize the activation energy of the MTM molecule. A cross-linking molecule which incorporates non-metal high-Z elements compared to the baseline xMT crosslinker, was introduced in the system for increased optical density in MTR Gen1. The photoacid generator was replaced in MTR Gen2.1 to optimize the ROP activation rate. Figure 1 depicts the evolution of the MTR generations. A photo-decomposable nucleophilic epoxy quencher is also added. [26] Variants of MTR Gen2 were obtained by modifying the components and the formulation ratios.

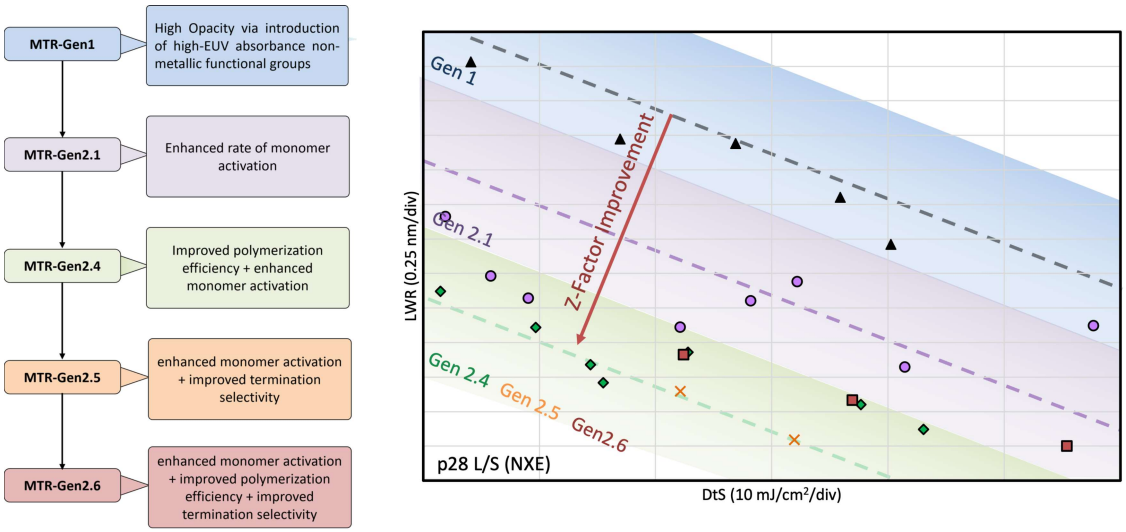

Figure 1: Schematic depicting the MTR evolution (left), together with indicative patterning performance (right). (Triangle - MTR Gen1; Circle - MTR Gen2.1; Diamond - MTR Gen 2.4, Cross – MTR Gen 2.5, Square - MTR Gen2.6). All data collected at p28 on the NXE3400.

3. RESULTS

3.1 Optimisation of MTR Gen2.4 for p32 hexagonal pillars

As noted previously, by varying the relative ratios of the MTR Gen2.4 components it is possible to produce a resist with higher or lower sensitivity, depending on the application requirements. This resist was patterned on a 5 nm thick bespoke organic underlayer (UL-2) at a spun film thickness of 21 nm. As shown in figure 2a, Gen 2.4 'Fast' can pattern p32 hexagonal pillars with a diameter of 15.8 nm at a dose of 42 mJ/cm^2, whilst Gen 2.4 'Slow' takes a dose of 72 mJ/cm^2 to pattern the same diameter (unbiased figures). The crucial question regards the impact of this dose difference on both the LCDU and defectivity of the pattern. The defectivity of these pillars will manifest as missing pillars in the underdosed region and touching pillars in the overdosed region. As shown in figure 2b, the unbiased LCDU values are very similar up to around 17nm pillar diameter, and are only 0.1nm different at 18 nm pillar diameter. The minimum LCDU is 2.3 nm for the 'slow' resist and 2.4 nm for the 'fast' resist. This metric by itself may suggest that the use of the faster resist is preferable. However, the defectivity, shown in figure 3, immediately shows that the slower resist has far fewer defects at all pillar diameters. This can be visually seen in the ADI pillar images as shown in figure 4. It should be noted that the Gen 2.4 'slow' resist has a minimum ADI defect fraction of 4.0×10^{-5} for a pillar diameter of 15.30 nm, and that the defect type is merged pillars rather than missing pillars.

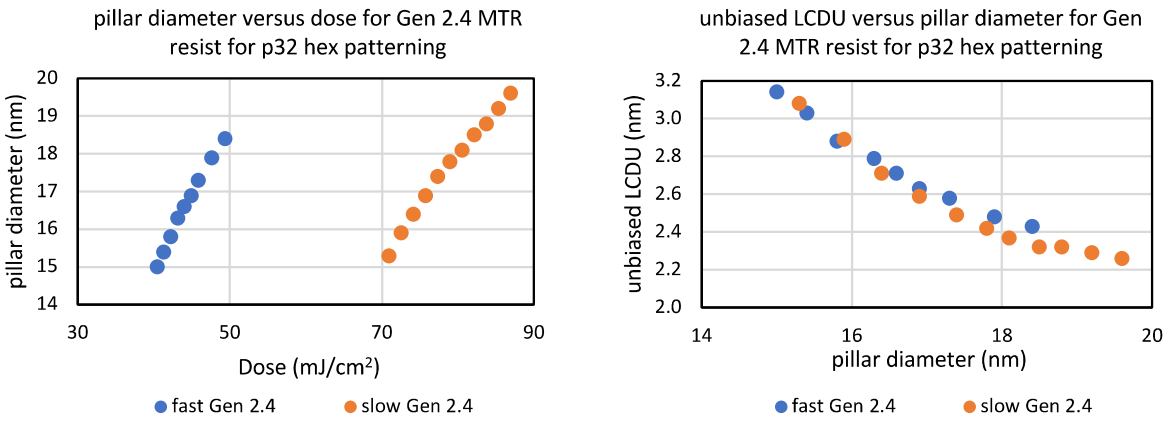

Figure 2a (left): Pillar diameter versus dose (measured via MetroLER) for 2 different Gen 2.4 resists. Figure 2b (right) unbiased LCDU as a function of pillar diameter (both measured via MetroLER) for 2 different Gen 2.4 resists. All exposures undertaken on the NXE3400, and with otherwise identical patterning and processing conditions.

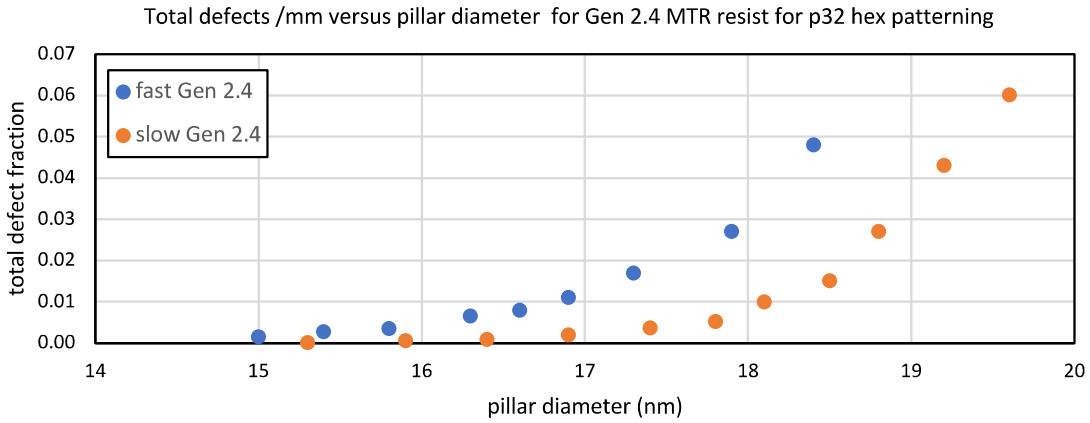

Figure 3 (left): Pillar diameter versus total defect fraction (measured via MetroLER) for 2 different Gen 2.4 resists. All exposures undertaken on the NXE3400, and with otherwise identical patterning and processing conditions.

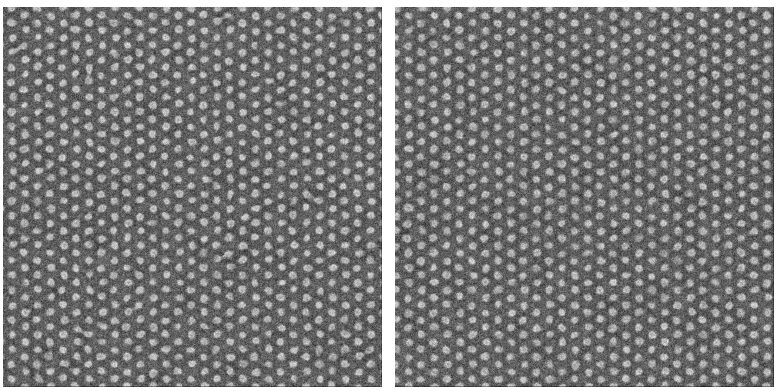

Figure 4: pillars patterned on the NXE3400 at p32 hex: (left) MTR Gen2.4 'fast', dose 43.1 mJ/cm²; diameter 16.3 nm, unbiased LCDU 2.79 nm; (right) MTR Gen2.4 'slow', dose 74.1 mJ/cm²; diameter 16.4 nm, unbiased LCDU 2.71 nm.

3.2 Optimisation of MTR Gen2.4 for p28 dense line/spaces

A similar experiment for dense line/spaces was carried out changing the formulation ratio to provide three different sensitivity resists, adding in a 'mid' sensitivity Gen 2.4. In addition to this, a Gen 2.1 resist with a dose midway between the Gen 2.4 'fast' and Gen 2.4 'mid' resist was patterned and compared. The spun film thickness for L/S was 20–22nm and no PEB was applied. The wafers all underwent MetroLER analysis and the unbiased LWR, LER and defectivity have been plotted. As seen in figure 5, the dose to achieve 14nm lines can be varied from 34 mJ/cm^2 to 58mJ/cm^2. The figure also shows that the slow Gen 2.4 has significantly lower LWR than the other samples, albeit at a higher dose.

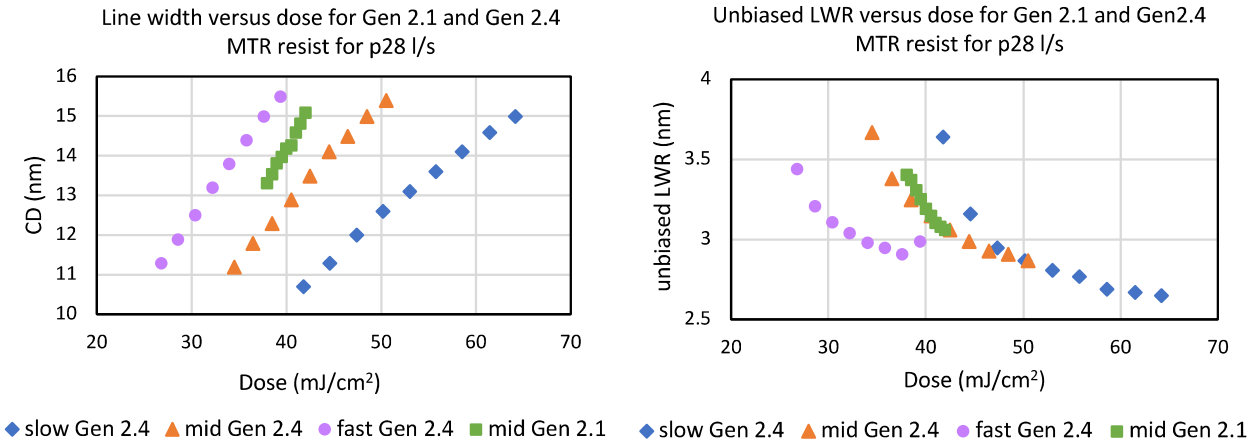

Figure 5 p28 L/S patterning in MTR Gen 2.1 and Gen 2.4; (left) line width versus dose; (right) Unbiased LWR versus dose. Exposed using the NXE3400 and analysed using MetroLER.

Examining figure 6, which shows unbiased LER versus line width, indicates that all generations of Gen 2.4 resist have lower roughness than the Gen 2.1 resist. The results also suggest that that the 'fast' Gen 2.4 resist gives similar roughness values to a resist ('mid' Gen 2.4) that requires 9mJ/cm^2 more dose. However, in a similar way to how dose affects the defectivity of pillars, for dense line/spaces less sensitive formulations show a wider the failure free window for defects, as also shown in figure 6. MetroLER analysis suggests that the failure free window for the 'slow' Gen 2.4 resist is at least from 12.0 nm to 13.6 nm (0 defects/mm) with <5 defects/mm between 11.3 nm and 14.6 nm linewidth (3.3 nm total window).

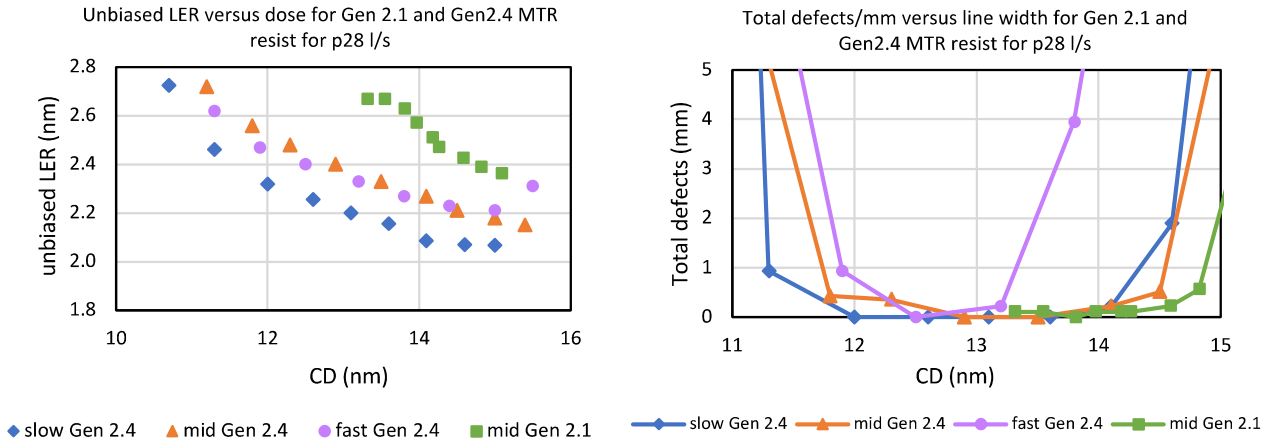

Figure 6: p28 L/S patterning in MTR Gen 2.1 and Gen 2.4: (left) Unbiased LER versus line width (right) Total defects per mm versus line width. Exposed using the NXE3400 and analysed using MetroLER.

3.3 Introduction of MTR Gen2.6 with comparison to Gen 2.4

Whilst Gen 2.4 resist combines changes which improve polymerization efficiency and enhanced monomer activation, Gen 2.6 also includes improved termination selectivity. Initial measurements for p32 pillars show that formulations that have a similar sensitivity, i.e. with the Gen 2.6 having a dose to size 9% higher than the slow Gen 2.4 resist, the LCDU can be reduced by 0.2nm (figure 7). Similarly, for p28 l/s, for a 15% increase in dose, the Gen 2.6 resist can pattern with a biased LWR around 0.3nm lower than Gen 2.4 (figure 7 and 8).

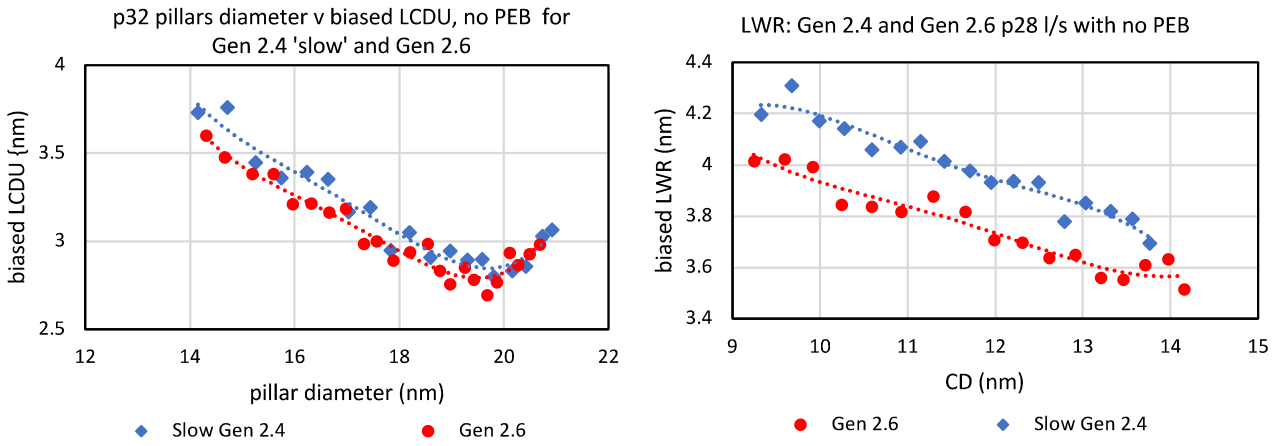

Figure 7: Patterning with Gen 2.6 resist and comparing to 'slow' Gen 2.4 resist on NXE3400: (left) p32 hex pillars, biased LCDU v pillar diameter; (right) p28 l/s, biased LWR versus line width

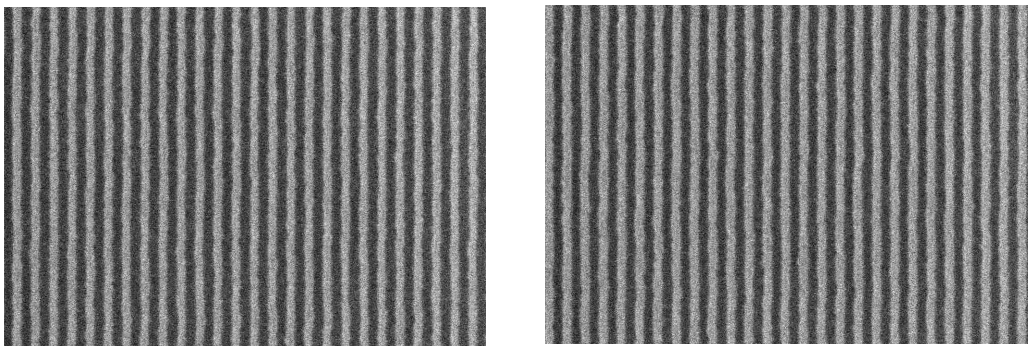

Figure 8: Patterning with Gen2.6 resist at p28 l/s on NXE3400, spun film thickness 22nm: (left) 64 mJ/cm^2; CD 11.96 nm, biased LWR 3.80 nm; (right) 69 mJ/cm^2, CD 12.93 nm, biased LWR 3.57 nm

3.4 Developer impact

A comparison of n-butyl acetate (nBA) and Fujifilm DP819A using 'production' wafers, i.e. patterned at the same dose and focus across the 300 mm wafer, shows that the nBA is a much more aggressive developer, reducing the line width by 1.5 nm compared to DP819A. The LWR and LER are on average 0.2 nm lower using DP819A across the production wafer (see figure 9). However, the range and standard deviation in line width and roughness is lower when using nBA. A further solvent change is likely to introduce more benefits such as reduced roughness and non-uniformity, and IM are currently investigating this.

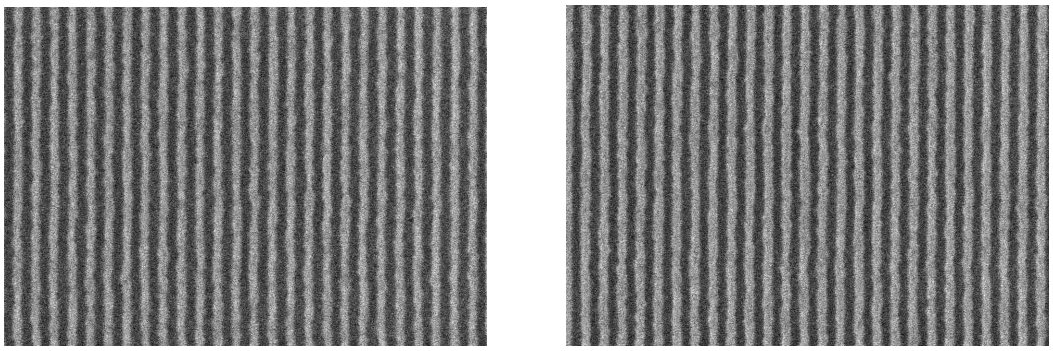

Figure 9: Patterning with Gen 2.4 resist at p28 l/s with 21 nm spun film thickness at 31 mJ/cm^2 on NXE3400, using a 65°C PEB and developed with different developers: (left) n butyl acetate: CD 11.5 nm, biased LWR 5.05 nm; (right) Fujifilm DP819A, CD 13.0 nm, biased LWR 4.85 nm

4. CONCLUSIONS

The lithographic performance of several MTR formulations was shown. By modifying the MTM molecule, crosslinker and PAG, both individually and in combination, we can optimize the reaction rates in the MTR mechanism. Different combinations have been designated Gen 2.1 to Gen 2.6 and show an LWR improvement in Gen 2.4 and 2.6 combinations. We presented the lithographic performance at pitch 28 nm dense line/space where 14.1 nm wide lines were patterned at 59 mJ/cm^2 with an unbiased LER of 2.09 nm using a Gen 2.4 resist. We showed hexagonal pillar results: pitch 32 nm patterned at 42 mJ/cm^2 to obtain a pillar diameter of 16 nm with an unbiased LCDU of 2.8 nm and additionally, p32 pillars of 16 nm diameter were patterned at 74 mJ/cm^2 with an unbiased LCDU of 2.7 nm, and of 18.5 nm diameter at 82 mJ/cm^2 with an unbiased LCDU of 2.3 nm. We also showed data which shows using a Gen 2.6 resist can reduce the LCDU of p32 hex pillars by 0.2 nm and biased LWR of p28 l/s by 0.3 nm compared to a comparable Gen 2.4 resist.

Performance improvements such as reduced roughness and defectivity can also be shown to be affected by choices such as underlayer and developer. We showed that the modification of the developer can be shown to influence the patterning performance of the resist at high resolution.

ACKNOWLEDGEMENTS

The authors thank Irresistible Materials Ltd. and Nano-C for support and provision of resist materials. The authors would like to thank Chris Mack and Bill Usry from Fractilia for providing MetroLER measurements, and to Roberto Fallica from imec also for MetroLER measurements.

REFERENCES

[1] Nagahara, S., Que Dinh, C., Yoshida, K., Shiraishi, G., Kondo, Y., Yoshihara, K., Nafus, K., Petersen, J.S., De Simone, D., Foubert, P., Vandenberghe, G., Stock, H-J, Meliorisz, B., "EUV resist chemical gradient enhancement by UV flood exposure for improvement in EUV resist resolution, process control, roughness, sensitivity, and stochastic defectivity," *Proc. SPIE*, **11326**, 113260A (2020).

[2] Shirotori, A., Hoshino, M., De Simone, D., Vandenberghe, G., Matsumoto, H., "A novel main chain scission type photoresists for EUV lithography", *Proc SPIE*, **11517**, 115170D (2020).

[3] Sharma, S.K., Kumar, R., Chauhan, M., Moinuddin, M.G., Peter, J., Ghosh, S., Pradeep, C.P., Gonsalves, K.E., "All-new nickel-based Metal Core Organic Cluster (MCOC) resist for N7+ node patterning," *Proc SPIE*, **11326**, 1132604 (2020).

[4] Torok, J., Del Re, R., Herbol, H., Das, S., Bocharova, I., Paolucci, A., Ocola, L. E., Ventrice Jr., C., Lifshin E., Denbeaux, G., Brainard, R. L., "Secondary Electrons in EUV Lithography," *J Photopolym. Sci. Technol.*, **26**, 625–634 (2013).

[5] Thackeray, J., Cameron, J., Jain, V., LaBeaume, P., Coley S., Ongayi O., Wagner M., Rachford A., Biafore J., "Progress in Resolution, Sensitivity and Critical Dimensional Uniformity of EUV Chemically amplified Resists," *Proc. SPIE*, **8682**, 868213 (2013).

[6] Nakano, A., Kozawa, T., Okamoto, K., Tagawa, S., Kai, T., Shimokawa, T., "Acid Generation Mechanism of Poly(4-hydroxystyrene)-Based Chemically Amplified Resists for Post-Optical Lithography: Acid Yield and Deprotonation Behavior of Poly(4-hydroxystyrene) and Poly(4-methoxystyrene)," *Jpn. J. App. Phys.,* **45**, 6866–6871 (2006).

[7] Narasimhan, A., Wisehart, L., Grzeskowiak, S., Ocola, L.E., Denbeaux, G., Brainard, R. L., "What we don't know about EUV exposure mechanisms," J Photopolym. Sci. Technol., **30**, 113–120 (2017).

[8] Long, L.T., Neureuther, A., Walraff, G., Naulleau, P. "Resist Underlayer Simulations," In *IEUVI TWG April 2022*, 7, (2022), http://ieuvi.org/TWG/Resist/IEUVI_Resist01.htm (Accessed 13/02/2023).

[9] Raley, A., Huli, L., Grzeskowiak, S., Lutker-Lee, K., Krawicz, A., Feurprier, Y., Liu, E., Kato, K., Nafus, K., Dauendorffer, A., Bae, N., LaRose, J., Metz, A., Hetzer, D., Honda, M., Nishizuka, T., Ko, A., Okada, S., Ido, Y., Onitsuka, T., Kawakami, S., Fujimoto, S., Shimura, S., Dinh, C.Q., Muramatsu, M., Biolsi, P., Mochiki, H. and Nagahara, S., "Outlook for high-NA EUV patterning: a holistic patterning approach to address upcoming challenges," *Proc SPIE*, **12056**, 120560A (2022).

[10] Severi, J., Lorusso, G.F., De Simone, D., Moussa, A., Saib, M., Duflou, R., De Gendta, S., "Chemically amplified resist CDSEM metrology exploration for high NA EUV lithography," *J Micro/Nanopattern. Mater. Metrol.*, **21**, 021207 (2022).

[11] Goldfarb, D.L., Bruce, R.L., Bucchignano, J.J., Klaus, D.P., Guillorn, M.A. and Wu, C.J., "Pattern collapse mitigation strategies for EUV lithography," *Proc SPIE,* **8322** (2012) 832205.

[12] Noga, D.E., Lawson, R.A., Lee, C.T., Tolbert, L.M. and Henderson, C.L., "Understanding pattern collapse in high-resolution lithography: impact of feature width on critical stress." *Proc* SPIE, **7273** (2009) 727334.

[13] Burov, A., Pret, A.V. and Gronheid, R., "Depth of focus in high-NA EUV lithography: a simulation study." *Proc SPIE,* **12293** (2022) 122930V.

[14] Fallica, R., De Simone, D., Chen, S., Safdar, M. and Suh, H.S., "Scaling and readiness of underlayers for high-NA EUV lithography," *Proc* SPIE, **12292**, 122920V (2022).

[15] Vesters, Y., McClelland, A., Popescu, C., Dawson, G., Roth, J., Theis, W., de Simone, D., Vandenberghe, G., Robinson, A.P.G, "Multi-trigger resist patterning with ASML NXE3300 EUV scanner," *Proc. SPIE*, **10586**, 1058308 (2018).

[16] Popescu, C., Kazazis, D., McClelland, A., Dawson, G., Roth, J., Theis, W., Ekinci, Y., Robinson, A.P.G., "High-resolution EUV lithography using a multi-trigger resist," *Proc SPIE*, 10583, 105831L (2018).

[17] O'Callaghan, G., Popescu, C., McClelland, A., Kazazis, D., Roth, J., Theis, W., Ekinici, Y., Robinson, A.P. G., "Multi-trigger resist – Novel synthesis improvements for high resolution EUV lithography," *Proc SPIE*, **10960**, 109600C (2019).

[18] Montgomery, W., McClelland A., Ure D., Roth J., Robinson A., "Irresistible Materials multi-trigger resist: the journey towards high volume readiness," *Proc SPIE*, **10143**, 1014328 (2017).

[19] Popescu, C., McClelland, A., Kazazis, D., Dawson, G., Roth, R., Ekinci, Y., Theis, W. and Robinson, A. P.G., "Multi-trigger resist for electron beam and extreme ultraviolet lithography," *Proc SPIE*, **10775**, 1077502 (2018).

[20] Popescu C., O'Callaghan G., McClelland A., Roth J., Lada T., Robinson A.P.G., "Performance enhancements with high opacity multi-trigger resist," *Proc SPIE*, **11326**, 1132611 (2020).

[21] Popescu, C., O'Callaghan, G., McClelland, A., Roth, J., Lada, T., Kudo, T., Dammel, R., Moinpour, M., Cao, Y., Robinson, A. P. G., "Progress in the multi-trigger resist," *Proc SPIE*, **11612**, 116120K (2021).

[22] Popescu, C., O'Callaghan, G., McClelland, A., Roth, J., Jackson, E., Robinson, A. P. G., "Component optimization in the multi-trigger resist," *Proc SPIE*, **12055**, 120550G (2022).

[23] Popescu, C., O'Callaghan, G., McClelland, A., Storey, C., Roth, J., Jackson, E. and Robinson, A.P.G., " Recent accomplishments in EUV lithography patterning for multi-trigger resist," *Proc SPIE*, **12292**, 122920E (2022).

[24] Popescu, C., O'Callaghan, G., McClelland, A., Storey, C., Roth, J., Jackson, E. and Robinson, A.P.G., " Recent accomplishments in EUV lithography patterning for multi-trigger resist," *Proc SPIE*, **12292** (2022) 122920E.

[25] Popescu, C., O'Callaghan, G., McClelland, A., Storey, C., Roth, J., Jackson, E. and Robinson, A.P.G., "EUV lithography patterning using multi-trigger resist," *Proc SPIE*, **12498** (2023) 1249812.

[26] Lawson, R.A., Frommhold, A., Yang, D.X., Robinson, A.P.G, "Negative-tone organic molecular resists," In *Frontiers of Nanoscience*: *Materials and Processes for Next Generation Lithography*, **Vol. 11**, Robinson A.P.G. and Lawson R.A. eds., (Oxford: Elsevier, 2016). pp. 223-317.